Check for updates

Design of 3-Phenylcoumarins and 3-Thienylcoumarins as Potent Xanthine Oxidase Inhibitors: Synthesis, Biological Evaluation, and Docking Studies

Antonella Fais[+],[a] Francesca Pintus[+],[a] Benedetta Era,[a] Sonia Floris,*[a] Amit Kumar,[b] Debapriyo Sarmadhikari,[c] Valeria Sogos,[d] Eugenio Uriarte,[e, f] Shailendra Asthana,[c] and Maria João Matos*[e]

Coumarin scaffold has proven to be promising in the development of bioactive agents, such as xanthine oxidase (XO) inhibitors. Novel hydroxylated 3-arylcoumarins were designed, synthesized, and evaluated for their XO inhibition and antioxidant properties. 3-(3′-Bromophenyl)-5,7-dihydroxycoumarin (compound **11**) proved to be the most potent XO inhibitor, with an IC_{50} of 91 nM, being 162 times better than allopurinol, one of the reference controls. Kinetic analysis of compound **11** and compound **5** [3-(4′-bromothien-2′-yl)-5,7-dihydroxycoumar-in], the second-best compound within the series (IC_{50} of 280 nM), has been performed, and both compounds showed a mixed-type inhibition. Both compounds present good antioxidant activity (ability to scavenge ABTS radical) and are able to reduce reactive oxygen species (ROS) levels in H_2O_2-treated cells. In addition, they proved to be non-cytotoxic in a Caco-2 cells viability assay. Molecular docking studies have been carried out to correlate the compounds' theoretical and experimental binding affinity to the XO binding pocket.

Introduction

Xanthine oxidase (XO, 1.17.3.2.) is the key enzyme in the catabolism of purines.[1] It catalyzes the oxidation of hypoxanthine to xanthine and then to uric acid, which is excreted in the urine. During these reactions, XO oxidizes the substrate by transferring electrons to oxygen molecules to form either superoxide anion or hydrogen peroxide. Due to the production of these reactive oxygen species (ROS), as by-products of the reaction, XO is considered a pro-oxidant enzyme and represents an important therapeutic target to reduce oxidative stress and the production of uric acid.[2] Overproduction or reduced excretion of uric acid leads to abnormal amounts of uric acid in the body, leading to gouty and the development of stones in the urinary tract.[3] Therefore, compounds that can inhibit XO may reduce both uric acid circulating levels and ROS production. Moreover, hyperuricemia is associated with other patho-

logical conditions such as atherosclerotic cardiovascular disease, chronic kidney disease and diabetes.[4,5] All these conditions increase the importance of finding new effective XO inhibitors.

Allopurinol and febuxostat are clinically useful XO inhibitors used in gout treatment. Allopurinol is a substrate for XO, which converts it to oxypurinol, which in turn inhibits XO.[6,7] However, allopurinol and febuxostat have serious side effects. Thus, new alternatives with increased therapeutic activity and lesser side effects are desired.[8,9]

In the last five years, we studied different compounds presenting the coumarin scaffold against the XO.[10,11] From the chemical point of view, we explored different aromatic groups at position 3 of the scaffold: phenyl, 2-thienyl (Figure 1), and 3-thienyl groups. We also explored the presence of different hydroxyl groups (number and position) in both the coumarin scaffold and/or the ring attached at position 3 (Figure 1). From a series of 28 different combinations, we identified the presence

[a] Prof. A. Fais,[+] Prof. F. Pintus,[+] Dr. B. Era, Dr. S. Floris
     Department of Life and Environmental Sciences
     University of Cagliari
     S.P. 8 km 0.700, 09042 Cagliari (Italy)
     E-mail: s.floris@unica.it

[b] Dr. A. Kumar
     Department of Electrical and Electronic Engineering
     University of Cagliari
     Via Marengo 2, 09123 Cagliari (Italy)

[c] Dr. D. Sarmadhikari, Dr. S. Asthana
     Translational Health Science and Technology Institute
     NCR Biotech Science Cluster
     Faridabad 121001 (India)

[d] Prof. V. Sogos
     Department of Biomedical Sciences
     University of Cagliari
     S.P. 8 km 0.700, 09042 Monserrato (Italy)

[e] Prof. E. Uriarte, Prof. M. J. Matos
     Departamento de Química Orgánica
     Facultade de Farmacia, Universidade Santiago de Compostela
     15782 Santiago de Compostela (Spain)
     E-mail: mm2147@cam.ac.uk

[f] Prof. E. Uriarte
     Instituto de Ciencias Químicas Aplicadas
     Universidad Autónoma de Chile
     7500912 Santiago (Chile)

[+] These authors contributed equally to this work.

     Supporting information for this article is available on the WWW under
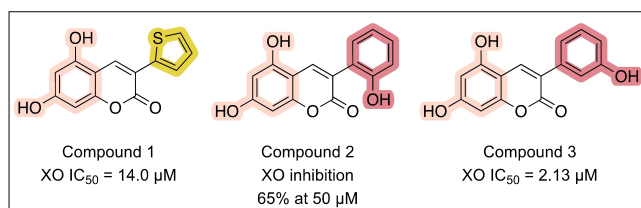   https://doi.org/10.1002/cmdc.202300400

Figure 1. Structures of three compounds with some previous data on XO inhibition that inspired the current study on dual antioxidant and XO inhibitors. Relevant chemical features are highlighted in different colours.

of two hydroxyl groups at positions 5,7 of the coumarin scaffold and one hydroxyl group at meta position of the 3-phenyl ring as the best spots to modulate the activity (Figure 1).
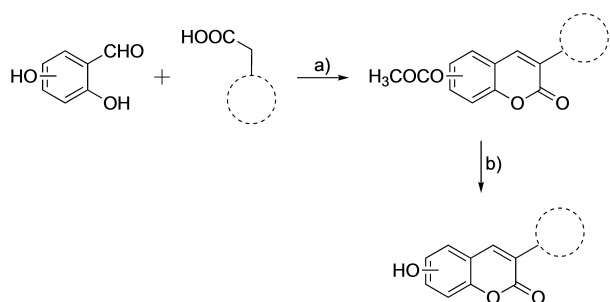
Additionally, simple coumarins and 3-arylcoumarins bearing hydroxyl groups have already proved to be interesting antioxidants.[12] The capacity to scavenge free radicals, combined with XO inhibition, has been described as a promising approach for hyperuricemia treatment.[13,14]

So far, compound **3** (Figure 1) has proved to be the best compound among all the molecules studied by the research group, with an IC_{50} against XO in the low micromolar range (2.13 μM). This compound, together with our knowledge on chemistry behind these molecules, inspired us to follow the pathway to discover new compounds with improved activity against this enzyme. We also explored the potential antioxidant activity of the designed molecules. Furthermore, molecular docking studies analyzed the interaction between the best compounds within the series and XO binding pocket.

Results and Discussion

Chemistry

Molecules 1–11 were obtained by Perkin-Oglialoro reaction, following the synthetic methodology presented in Scheme 1. This reaction is one of the best alternatives to synthesize hydroxyl modified 3-phenyl- or 3-thienylcoumarins, occurring in two consecutive steps. In the first moment, acetoxylated derivatives are synthesized, followed by acidic hydrolysis that allows obtaining the correspondent hydroxyl derivatives. For the first step, *ortho*-hydroxybenzaldehydes and phenylacetic or thienylacetic acids react for 16 hours, at reflux temperature, in the presence of potassium acetate (CH_3CO_2K) and acetic anhydride (Ac_2O). These mild conditions allow the concomitant acetylation of the hydroxyl groups on the scaffold and the closure of the pyrone ring. Acetoxylated derivates then undergo hydrolysis in the presence of aqueous hydrochloric acid (HCl) and methanol (MeOH), at reflux temperature, for 3 hours. Hydroxyl substituted 3-phenyl- or 3-thienylcoumarins (1–11) are then obtained in high yields. The success of the first reaction is confirmed by the presence of a peak corresponding to the H-4 around 8 ppm in the ^1H NMR. The success of the second reaction is confirmed by the disappearance of peaks corresponding to the acetylated counterparts between 2 and 3 ppm, and the appearance of peaks corresponding to the hydroxyl groups between 9 and 11 ppm in the ^1H NMR.

Biological assays

The effect of the novel compounds **4–11** on the XO activity has been tested, and the IC_{50} values have been calculated and compared to the previously described compounds **1–3**[10] (Table 1).

From the studied series, two compounds presented activity against XO in the nanomolar range (Table 1). 3-(4'-Bromothien-2'-yl)-5,7-dihydroxycoumarin (**5**), the second-best compound within the series, inhibits the XO with an IC_{50} of 280 nM. 3-(3'-Bromophenyl)-5,7-dihydroxycoumarin (**11**), the best XO inhibitor (IC_{50} of 91 nM), proved to be 153 times better than 5,7-dihydroxy-3-(thien-2'-yl)coumarin (**1**), 23 times better than 5,7-

Scheme 1. Synthetic methodologies and reaction conditions: a) CH_3CO_2K, Ac_2O, reflux, 16 h; b) HCl, MeOH, reflux, 3 h.

4. 5,7-dihydroxy and 3-thienyl
5. 5,7-dihydroxy and 4-bromo-2-thienyl
6. 6,7-dihydroxy and 3-thienyl
7. 6,7-dihydroxy and 4-bromo-2-thienyl
8. 6,7-dihydroxy and 3-hydroxyphenyl
9. 6,7-dihydroxy and 3-bromophenyl
10. 7,8-dihydroxy and 3-bromophenyl
11. 5,7-dihydroxy and 3-bromophenyl

Table 1. IC_{50} values of 3-aryl and 3-heteroarylcoumarin derivatives against XO.

Compound	IC_{50} [μM][a]
1	14.00 ± 0.65
2	4.49 ± 0.8
3	2.13 ± 0.27
4	5.49 ± 0.10
5	0.28 ± 0.08
6	10.75 ± 1.64
7	28.50 ± 0.66
8	28.64 ± 0.90
9	8.28 ± 0.23
10	25.22 ± 1.10
11	0.091 ± 0.003
Allopurinol	14.75 ± 1.03
Febuxostat	0.020[15]

[a] Data are the mean ± standard deviation (SD) of three independent experiments.

dihydroxy-3-(3′-hydroxyphenyl)coumarin (**3**), and 162 times better than allopurinol, the reference compound (its IC_{50} value was calculated in the same experimental conditions). The best compound within the series shows an IC_{50} value in the nanomolar range, as febuxostat. Structurally, compound **1** presents a 2-thienyl group at position 3 of the coumarin scaffold and compound **3** a 3-hydroxyphenyl group at the same position of the coumarin scaffold. It is interesting to notice that the change of a bromine (compound **11**) for a hydroxyl (compound **3**) at the same position dramatically changes the activity. Comparing compounds **1** and **5**, the introduction of a bromine at the 2-thienyl ring at position 3 of the coumarin scaffold increased the activity 120 times. Therefore, it looks that the presence of a halogen, an electronegative and electron withdrawing group, creates an inductive effect important for the described activity.

Since compounds **5** and **11** showed the best inhibitory activity among the compounds of this series, and they also exerted a more potent inhibition if compared with the standard molecule, we, therefore, focused our attention on these two compounds. To evaluate the mode of inhibition, we investigated the kinetic behaviour of XO at different concentrations of substrate and compounds by Lineweaver-Burk plot analysis. Kinetic analysis revealed that both compounds **5** and **11** act as mixed-type inhibitors. In fact, increasing the inhibitor concentration resulted in a family of straight lines with different slopes and intercepts (Figures 2 and 3). This behaviour is characteristic of a mixed-type inhibitor which can bind the free enzyme and also the enzyme-substrate complex. The equilibrium constants for binding with the free enzyme (K_I) and with the enzyme-substrate complex (K_{IS}) have been obtained either from the slope (K_m/V_{max}) or the $1/V_{max}$ values plotted *versus* the inhibitor concentration, respectively. The values of K_I and K_{IS} of compound **5** proved to be 0.12 μM and 0.22 μM, respectively. The values of K_I and K_{IS} of compound **11** proved to be 28.51 nM and 60.96 nM, respectively.

The antioxidant properties of compounds have been evaluated by ABTS radical scavenging assay, and the results are reported in Table 2. Antioxidant activity is expressed as EC_{50}, and the values have been compared with the EC_{50} of the positive control, Trolox. All the compounds possess an ability to quench ABTS radical. Compounds **5** and **11**, which show the best XO inhibitory properties, also possess a good antioxidant activity with EC_{50} of 11.69 and 19.54 μM, respectively.

MTT assay has been performed using Caco-2 cells to understand the potential effect on cell viability of compounds **5** and **11**. Notably, these compounds are non-cytotoxic at the studied concentrations (Figure 4A). Then, cellular experiments have been carried out to evaluate ROS levels in the cells before and after oxidative stress induction, and after treatment with compounds **5** or **11**. The assay is based on the use of the
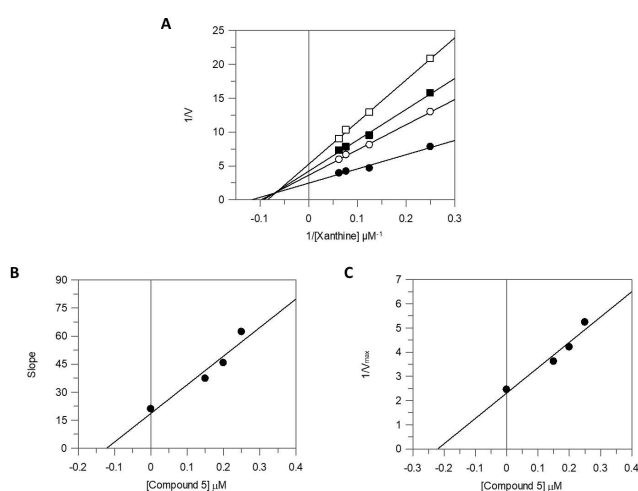
Figure 2. Inhibition of XO activity by compound **5**. **A**. Lineweaver-Burk plot. The concentrations of inhibitor were 0 (●), 0.15 (○), 0.2 (■), and 0.25 (□) μM. **B**. and **C**. The secondary plot of slope (K_m/V_{max}) *versus* compound concentration (**A**) and the secondary plot of $1/V_{max}$ *versus* compound concentration (**B**).

Figure 3. Inhibition of XO activity by compound **11**. **A**. Lineweaver-Burk plot. The concentrations of inhibitor were 0 (○), 25 (●), 50 (□), and 75 (■) nM. **B**. and **C**. The secondary plot of slope (K_m/V_{max}) *versus* compound concentration (**A**) and the secondary plot of $1/V_{max}$ *versus* compound concentration (**B**).
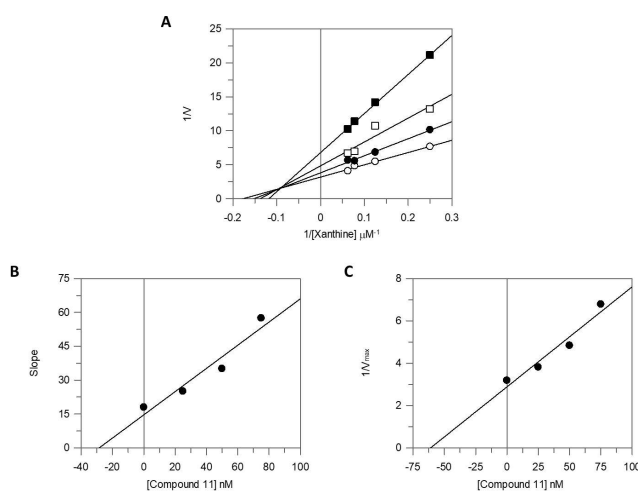
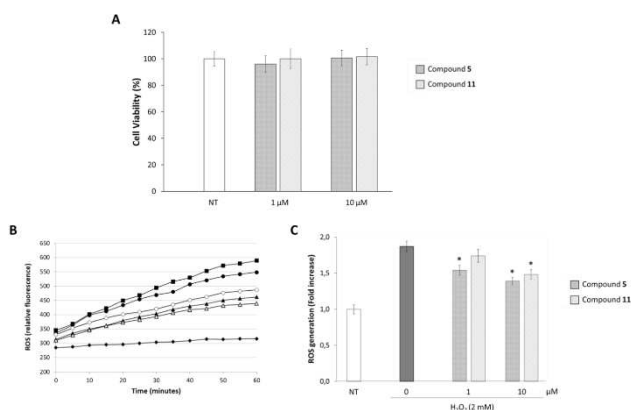| Table 2. Antioxidant activity of compounds 1–11.	
Compound	EC_{50} [μM][a]
1	8.51 ± 1.70[16]
2	20.62 ± 0.19
3	8.62 ± 0.18[12]
4	8.40 ± 0.20
5	11.69 ± 3.83
6	13.20 ± 1.46
7	38.97 ± 2.17
8	12.30 ± 1.30
9	16.03 ± 1.17
10	17.37 ± 0.54
11	19.54 ± 0.03
Trolox[b]	5.28 ± 0.15
[a] Data are the mean ± standard deviation (SD) of three independent experiments. [b] Reference compound.	

ChemMedChem

Research Article
doi.org/10.1002/cmdc.202300400

Chemistry
Europe
European Chemical
Societies Publishing

Figure 4. Effect of compounds **5** and **11** on Caco-2 cell viability (**A**) and inhibition of H_2O_2-induced ROS generation by compounds **5** and **11** on Caco-2 cells (**B** and **C**). **A**. Cell viability has been determined by an MTT assay after 24 hours of incubation with the compounds at different concentrations. **B**. ROS levels (expressed as DCF fluorescence) in cells pretreated with compounds and incubated with 2 mM of H_2O_2 up to 60 minutes. (♦): untreated cells, (■): 2 mM H_2O_2, (●): 10 μM Compound **11** + H_2O_2; (○) 1 μM Compound **11** + H_2O_2; (▲)10 μM Compound **5** + H_2O_2; (△): 1 μM Compound **5** + H_2O_2. **C**. Effect of compound **5** and **11** on ROS production in Caco-2 cells after 60 minutes treatment with 2 mM H_2O_2. Data (means ± SD) are normalized to untreated controls. *$p < 0.001$ compared to the H_2O_2 treated group.

Figure 5. The best docking poses of compounds **5** and **11** superimposed with ligand MTE (in cyan), with the binding site region within (3.5 Å) residues from MTE. The compounds are shown in white, rendered in licorice and colored by atom wise: nitrogen atom in blue, sulfur in yellow, hydrogen in white, oxygen in red and bromine in purple. The protein is represented in ghost view, rendered in cartoon and the binding site is shown by dotted lines. Docking outcomes of compounds **5** and compound **11** obtained, illustrating the interacting residues in licorice and in surface mode, respectively, within 3.5 Å from the ligands.

fluorescent dye 2′,7′-dichlorofluorescein diacetate (DCFH-DA), which easily passes through the cell membrane and is hydrolyzed by the intracellular esterases to DCFH. This can be further oxidized by intracellular ROS, with the formation of the highly fluorescent molecule DCF. The measurement of the fluorescence allows monitoring the amount of intracellular ROS during the experimental conditions. As shown in Figure 4B and 4C, H_2O_2 incubation significantly increased ROS formation in Caco-2 cells. A reduction in fluorescence was observed after the treatment of cells with compounds **5** or **11**. This means that both these compounds were able to inhibit H_2O_2-induced ROS production in a dose-response manner. Thus, these results confirm the previous antioxidant assay, and suggest that compounds **5** and **11** may reduce the formation of intracellular ROS.

Molecular docking

To gain insights into the observed *in vitro* activity of the best 3-phenyl and 3-thienylcoumarins, we used molecular docking to visualize the interactions of the compounds with the XO binding pocket (Figure 5). We performed the comparison of the binding mode of four compounds (**1**, **3**, **5** and **11**) with the MTE co-crystal ligand. Since the new set (compounds **5** and **11**) binds in the same pocket than the previously studied series (compounds **1** and **3**), the focused docking has been performed to enrich the binding pose and number of conformations. Compound **11** has been the most promising candidate, followed by compound **5**. The residues that may interact with compound **5** are Q112, C150, G796, G797, F798, R912, M1038, G1039, Q1194 and G1260 (Figure 5). For compound **11**, the
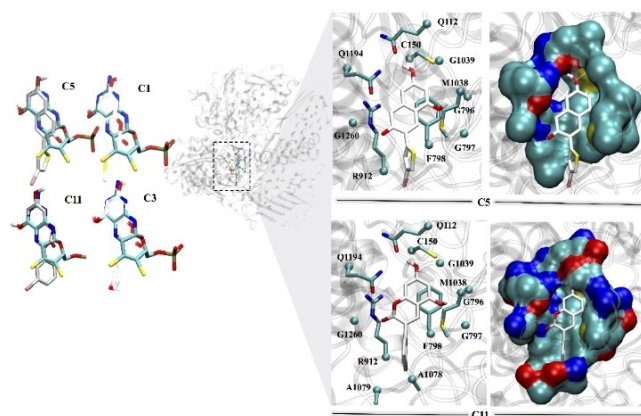
binding site residues are mainly similar, except for two alanine residues (A1078 and A1079), which help pack the binding site more nicely than for compound **5** (Figure 5). Molecular docking energy values, as well as the number of conformations for each compound, are summarized in Table 3.

Comparison between compounds **1** and **5** indicates that the presence of a bromine atom in the thienyl ring at position 3 of compound **5** results in a better docking energy value, as well as a higher number of conformations. Comparing compounds **3** and **11**, the presence once again of a bromine atom at the phenyl ring at position 3 of compound **11**, instead of a hydroxyl group at the same position of compound **3**, results in a better docking energy value along with a higher number of conformations. Among the four investigated compounds, the docking energy and number of conformations for top-ranked compounds **11** and **5** are −10.2 kcal/mol and 191, and −9.2 kcal/mol and 136, respectively, which suggests that compound **11** is a better candidate to be further explored.

Traditional XO inhibitors have three main structural components: a carboxyl group or heterocyclic aromatic moiety that may interact with Arg880 and Thr1010 through hydrogen bonds, a cyano or tetrazole substituted phenyl ring that may establish hydrogen bonds with Asn768, and a five-membered heterocyclic or amide as the linker, inspired in both febuxostat

Table 3. Molecular docking values of compounds **1**, **3**, **5** and **11**, along with the number of conformations found for each compound.

Compound	Docking energy [kcal/mol]	No. of conformations
1	−7.9	65
3	−9.0	78
5	−9.2	136
11	−10.2	191

ChemMedChem

Research Article
doi.org/10.1002/cmdc.202300400

Chemistry
Europe
European Chemical
Societies Publishing

and topiroxostat. In this work, engineering XO inhibitors by incorporating five-membered heteroaromatic rings in a well know scaffold have been explored, trying to open the chemical space of the traditionally know XO inhibitors.

Conclusions

We have designed and synthesized novel hydroxylated 3-phenyl and 3-thienylcoumarins, and evaluated them for their XO inhibition and antioxidant properties. The main goal of this study was to compare both series, based on previous data from the group. Compounds **11** and **5**, with lower IC_{50} values, have been studied for their kinetic profile, showing mixed-type inhibition patterns. Notably, both compounds present a bromine atom on the ring present at position 3 of the scaffold. This may indicate that, despite of the nature of that ring, the halogen presence and/or position is crucial for the activity. In addition, these compounds proved to be non-cytotoxic against the Caco-2 cell line, as well as good antioxidants on ABTS scavenging assays. In addition, these compounds reduced intracellular ROS levels in H_2O_2-treated cells. Both compounds have been further explored by *in silico* molecular docking studies. The docking energy and number of conformations suggest that compound **11** is the most promising candidate to be further explored. This research project can be a starting point for further investigation on the multitarget potential of these compounds. The promising results open the door to further challenges such as more extensive research on the pharmacological mechanisms and *in vivo* studies.

Experimental Section

Synthesis of compounds 1–11. Acetoxy-3-phenylcoumarins or Acetoxy-3-thienylcoumarins were synthesized under anhydrous conditions, using material previously dried at 60 °C for at least 12 h and at 300 °C for few minutes immediately before use. A solution containing anhydrous CH_3CO_2K (2.94 mmol), phenylacetic or thienylacetic acid (1.67 mmol), and the corresponding hydroxysalicylaldehyde (1.67 mmol), in Ac_2O (1.2 mL), was refluxed for 16 h. The reaction mixture was cooled, neutralized with 10% aqueous $NaHCO_3$, and extracted with EtOAc (3×30 mL). The organic layers were combined, washed with distilled water, dried (anhydrous Na_2SO_4), and evaporated under reduced pressure. The product was purified by recrystallization in EtOH and dried to afford the desired compound. Compounds **1–11** were obtained by hydrolysis of their acetoxylated counterparts, respectively. The appropriate acetoxylated coumarin, mixed with 2 N aqueous HCl and MeOH, was refluxed during 3 h. The resulting reaction mixture was cooled in an ice-bath and the reaction product, obtained as solid, was filtered, washed with cold distilled water, and dried under vacuum to afford the desired compound.

Biological activities. The antioxidant activity of the compounds was estimated by the ABTS assay, following the previously reported method.[17] The results are expressed as the concentration of sample necessary to give a 50% reduction in the original absorbance (EC_{50}).

Inhibition of XO activity was determined spectrophotometrically by monitoring the formation of uric acid at 295 nm. XO activity was measured following the previously reported method.[10] The inhib-

ition potency is expressed as IC_{50} values, which represent the inhibitor concentration giving 50% inhibition of enzyme activity.

Kinetic analysis of XO activity in the presence of the most promising compounds was determined by the Lineweaver-Burk double reciprocal plot in order to determine the mode of inhibition. The equilibrium constants for binding with the free enzyme (K_I) and with the enzyme-substrate complex (K_{IS}) have been obtained either from the slope (K_m/V_{max}) or the $1/V_{max}$ values plotted *versus* the inhibitor concentration, respectively.

Cell viability was detected by the colorimetric 3-(4,5-dimethylthiazol-2-yl)-2,5-diphenyltetrazolium bromide (MTT) assay, as previously described.[18]

The cellular ROS levels were determined following the 2′,7′-dichlorofluorescein diacetate (DCFH-DA) method.[18] Caco-2 cells were treated with different concentrations of the studied compounds and the fluorescence intensity was measured using a fluorescent plate reader at an excitation wavelength of 485 nm and emission wavelength of 530 nm.

Computational studies. The crystal structure for the XO enzyme (PDB ID: 1FIQ) was selected for molecular docking experiments. As part of our previous research[10] and provided as Supporting Information, we used AutoDock tools for docking and post-processing analysis.

Supporting Information

Additional references are cited within the Supporting Information.[19–25]

Conflict of Interests

The authors declare no conflicts of interest.

Data Availability Statement

The data that support the findings of this study are available from the corresponding author upon reasonable request.

[1] M. Bortolotti, L. Polito, M. G. Battelli, A. Bolognesi, *Redox Biol.* **2021**, *41*, 101882.
[2] R. Rullo, C. Cerchia, R. Nasso, V. Romanelli, E. De Vendittis, M. Masullo, A. Lavecchia, *Antioxidants* **2023**, *12*, DOI 10.3390/antiox12040825.
[3] B. T. Emmerson, *Drug Ther.* **1996**, *334*, 445–451.

[4] J. Chen, J. Ge, M. Zha, J. J. Miao, Z. L. Sun, J. Y. Yu, *Front. Endocrinol.* **2020**, *11*, DOI 10.3389/fendo.2020.00577.

[5] Y. Saito, A. Tanaka, K. Node, Y. Kobayashi, *J. Cardiol.* **2021**, *78*, 51–57.

[6] I. J. Anderson, A. M. Davis, R. H. Jan, *Jama* **2021**, *326*.

[7] C. M. Burns, R. L. Wortmann, *Ther. Adv. Chronic Dis.* **2012**, *3*, 271–286.

[8] U. G. Knaus, *Reactive Oxygen Species* **2018**.

[9] H. K. Gulati, K. Bhagat, A. Singh, N. Kumar, A. Kaur, A. Sharma, S. Heer, H. Singh, J. V. Singh, P. M. S. Bedi, *Med. Chem. Res.* **2020**, *29*, 1632–1642.

[10] A. Fais, B. Era, S. Asthana, V. Sogos, R. Medda, L. Santana, E. Uriarte, M. J. Matos, F. Delogu, A. Kumar, *Int. J. Biol. Macromol.* **2018**, *120*, 1286–1293.

[11] B. Era, G. L. Delogu, F. Pintus, A. Fais, G. Gatto, E. Uriarte, F. Borges, A. Kumar, M. J. Matos, *Int. J. Biol. Macromol.* **2020**, *162*, 774–780.

[12] M. J. Matos, C. Varela, S. Vilar, G. Hripcsak, F. Borges, L. Santana, E. Uriarte, A. Fais, A. Di Petrillo, F. Pintus, B. Era, *RSC Adv.* **2015**, *5*, 94227–94235.

[13] M. Gliozzi, N. Malara, S. Muscoli, V. Mollace, *Int. J. Cardiol.* **2016**, *213*, 23–27.

[14] N. A. A. Shukor, A. Ablat, N. A. Muhamad, J. Mohamad, *Int. J. Food Sci. Technol.* **2018**, *53*, 1476–1485.

[15] R. Kumar, Darpan, S. Sharma, R. Singh, *Expert Opin. Ther. Pat.* **2011**, *21*, 1071–1108.

[16] F. Pintus, M. J. Matos, S. Vilar, G. Hripcsak, C. Varela, E. Uriarte, L. Santana, F. Borges, R. Medda, A. Di Petrillo, B. Era, A. Fais, *Bioorg. Med. Chem.* **2017**, *25*, 1687–1695.

[17] S. Mirabile, M. P. Germanò, A. Fais, L. Lombardo, F. Ricci, S. Floris, A. Cacciola, A. Rapisarda, R. Gitto, L. De Luca, *ChemMedChem* **2022**, *17*, 1–14.

[18] B. Era, S. Floris, V. Sogos, C. Porcedda, A. Piras, R. Medda, A. Fais, F. Pintus, *Plants* **2021**, *10*, 1–12.

[19] R. O. Juvonen, E. M. Jokinen, A. Javaid, M. Lehtonen, H. Raunio, O. T. Pentikäinen, *Chem. Biol. Drug Des.* **2020**, *95*, 520–533.

[20] M. Valiev, E. J. Bylaska, N. Govind, K. Kowalski, T. P. Straatsma, H. J. J. Van Dam, D. Wang, J. Nieplocha, E. Apra, T. L. Windus, W. A. De Jong, *Comput. Phys. Commun.* **2010**, *181*, 1477–1489.

[21] A. Kumar, R. Cardia, G. Cappellini, *Cellulose* **2018**, *25*, 2191–2203.

[22] A. Kumar, G. Cappellini, F. Delogu, *Cellulose* **2019**, *26*, 1489–1501.

[23] O. A. J. Trott, Oleg, *J. Comput. Chem.* **2009**, *31*, 455–461.

[24] P. Caboni, B. Liori, A. Kumar, M. L. Santoru, S. Asthana, E. Pieroni, A. Fais, B. Era, E. Cacace, V. Ruggiero, L. Atzori, *PLoS One* **2014**, *9*, 1–8.

[25] M. Srivastava, L. Mittal, D. Sarmadhikari, V. K. Singh, A. Fais, A. Kumar, S. Asthana, *Pharmaceuticals* **2023**, *16*, DOI 10.3390/ph16030376.